Magnetism and Electronic State of Iron Ions on the Surface and in the Core of TiO_2 Nanoparticles

Anatoly Ye. Yermakov [1,2,*], Mikhail A. Uimin [1], Danil W. Boukhvalov [3,4], Artem S. Minin [1,2,*], Nadezhda M. Kleinerman [1], Sergey P. Naumov [1,2], Aleksey S. Volegov [1,2], Denis V. Starichenko [1], Kirill I. Borodin [1,2], Vasily S. Gaviko [1,2], Sergey F. Konev [4] and Nikolay A. Cherepanov [5]

1 M.N. Mikheev Institute of Metal Physics of Ural Branch of Russian Academy of Sciences, 620108 Ekaterinburg, Russia; mich.uymin@gmail.com (M.A.U.); kleinerman@imp.uran.ru (N.M.K.); naumov_sp@imp.uran.ru (S.P.N.); alexey.volegov@urfu.ru (A.S.V.); starichenko@imp.uran.ru (D.V.S.); bkimm@mail.ru (K.I.B.); gaviko@imp.uran.ru (V.S.G.)
2 Institute of Natural Sciences and Mathematics, Ural Federal University, 620083 Ekaterinburg, Russia
3 College of Science, Institute of Materials, Physics and Chemistry, Nanjing Forestry University, Nanjing 210037, China; danil@njfu.cn
4 Theoretical Physics and Applied Mathematics Department, Ural Federal University, 620002 Ekaterinburg, Russia; ksf50@bk.ru
5 Educational and Scientific Center for Expertise of Certification and Quality Problems, Ural Federal University, 620002 Ekaterinburg, Russia; n.a.cherepanov@urfu.ru
* Correspondence: yermakov.anatoly@gmail.com (A.Y.Y.); calamatica@gmail.com (A.S.M.)

1. XRD

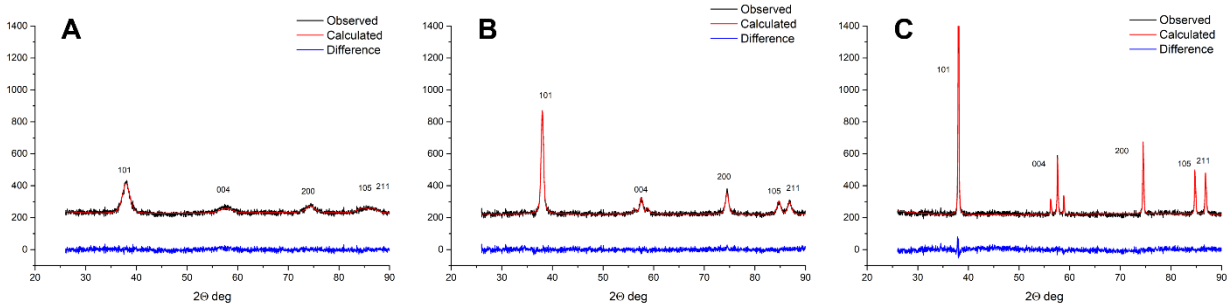

Figure S1 XRD of different initial TiO_2 samples taken in CrKα radiation. A – ST-01, B – ST-21, C – ST-41

All diffraction peaks correspond to TiO_2 in crystalline modification of anatase, no extraneous phases were detected.

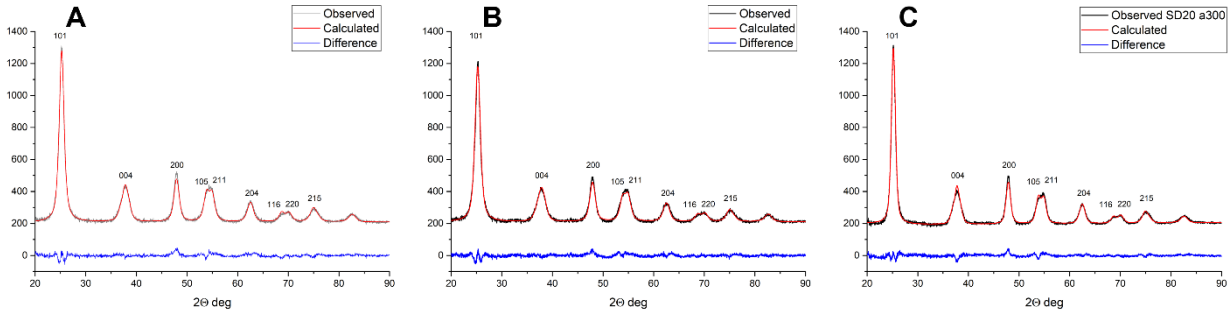

Figure S2 XRD of different initial TiO_2 samples taken in CuKα radiation. A – ST-01, B – ST-01 after deposition of iron ions and treatment with HCl, C – ST-01 after deposition of iron ions, annealing at 300° C in air, treatment with hydrochloric acid and sodium dithionite

After deposition of iron ions and subsequent treatment with hydrochloric acid, no new phases are observed. Similarly, and at annealing in air at a temperature of 300° C degrees with subsequent treatment with hydrochloric acid and sodium dithionite.

2. Transmission electron microscopy images

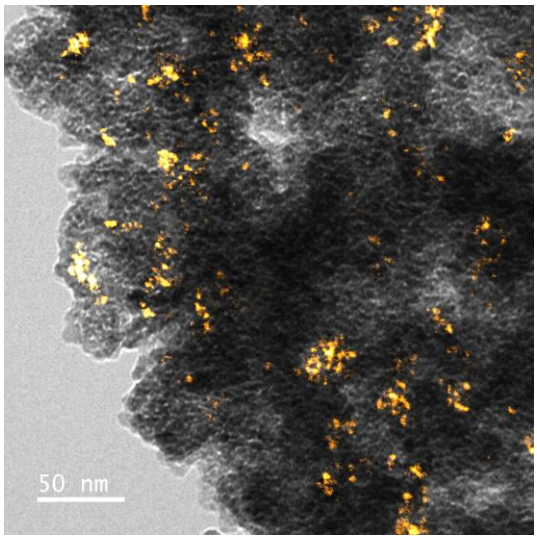

Figure S3 Brightfield (grayscale) and overlapped darkfield (yellow) images of ST-01 nanoparticles

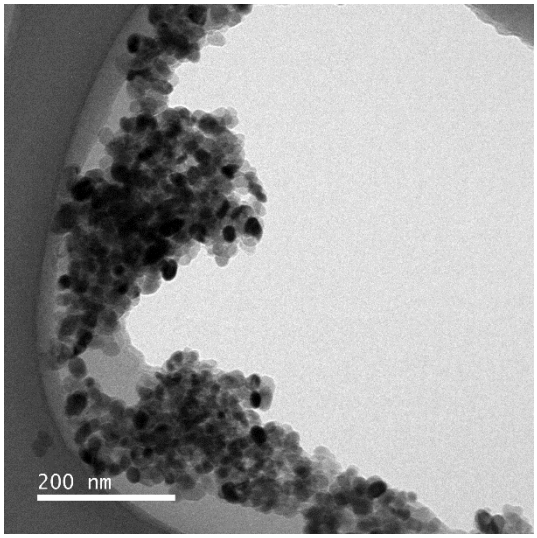

Figure S4. Brightfield (grayscale) image of ST-21 nanoparticles

3. IR spectroscopy

The IR spectrum of TiO_2 nanoparticles shows characteristic features for this material, including a peak from the Ti-O-Ti bond in the region of 600 cm^{-1} and Ti-O in the region of 480 cm^{-1}, as well as a broad signal from water (-OH and H-O-H) sorbed on the particle surface in the region of 3000 cm^{-1} and 1600 cm^{-1}, correspondingly. The signals just above 1500 cm^{-1} in initial samples (S 5), presumably, can be ascribed to hydroxyl groups. Moreover, the signal persists after HCl treatment, indicating that TiO_2 nanoparticles begin to interact with environmental after etching.

After sorption on the surface of iron ions is added signal in the region of 1500 cm^{-1} corresponding to Fe-OH, which disappears after treatment of particles with hydrochloric acid.

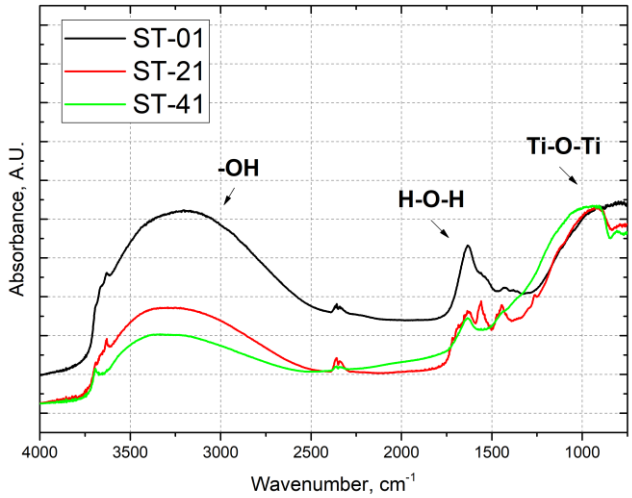

Figure S5 FTIR of titanium dioxide samples.

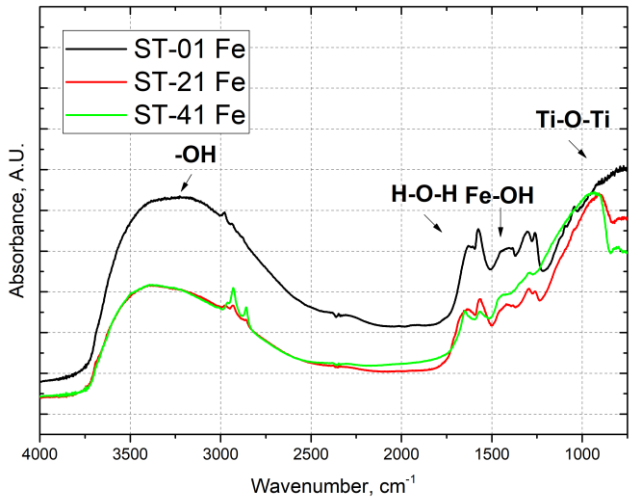

Figure S6 FTIR of titanium dioxide samples with iron ions deposited on the surface.

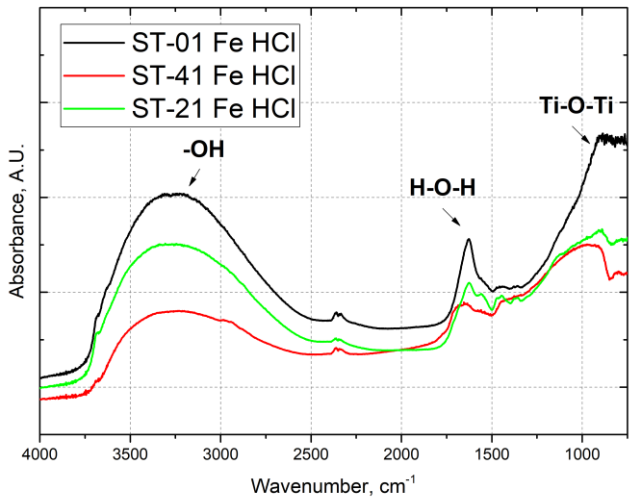

Figure S7 FTIR of titanium dioxide samples with iron ions deposited on the surface after HCl treatment.

4. Study of the effects of annealing after metal ion deposition by EPR spectroscopy

ST-01

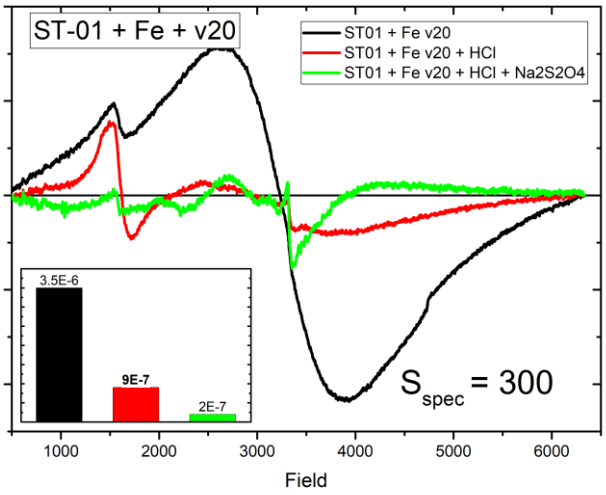

Figure S8 EPR spectra of samples prepared from ST-01 at different stages of the process, vacuum dried at room temperature. The inset shows the magnetic susceptibility of the sample.

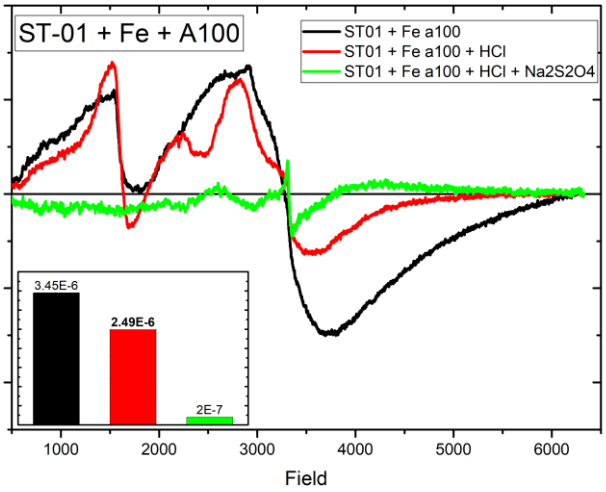

Figure S9 EPR spectra of samples prepared from ST-01 at different stages of the process, vacuum annealed at 100° C. The inset shows the magnetic susceptibility of the sample.

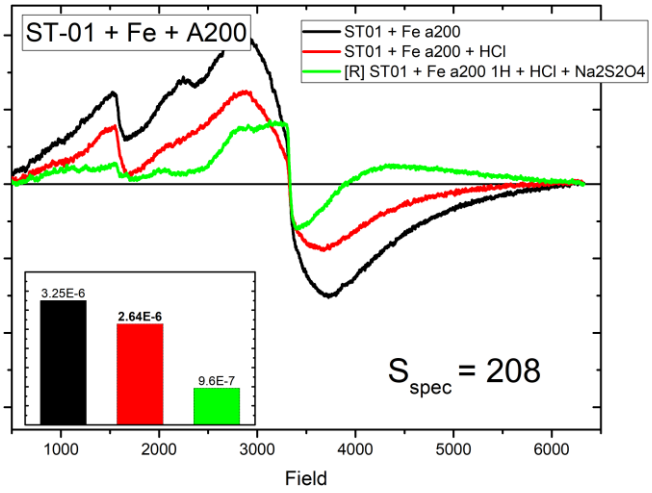

Figure S101 EPR spectra of samples prepared from ST-01 at different stages of the process, vacuum annealed at 200° C. The inset shows the magnetic susceptibility of the sample.

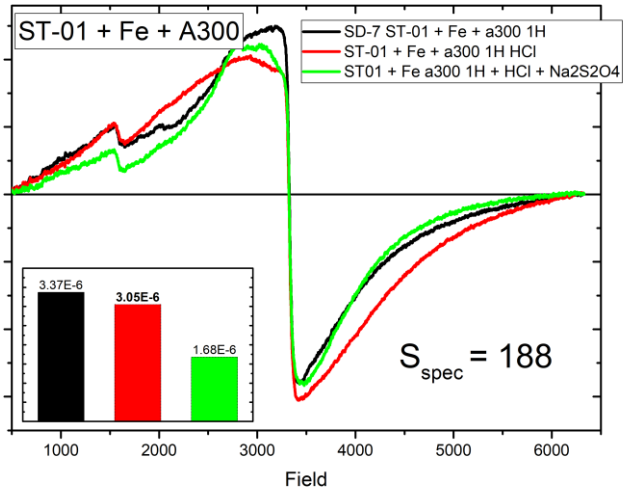

Figure S11 EPR spectra of samples prepared from ST-01 at different stages of the process, vacuum annealed at 300° C. The inset shows the magnetic susceptibility of the sample.

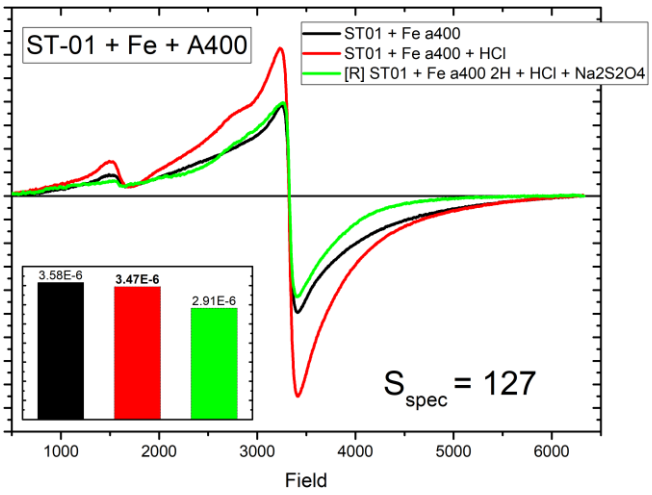

Figure S2 EPR spectra of samples prepared from ST-01 at different stages of the process, vacuum annealed at 400° C. The inset shows the magnetic susceptibility of the sample.

ST-21

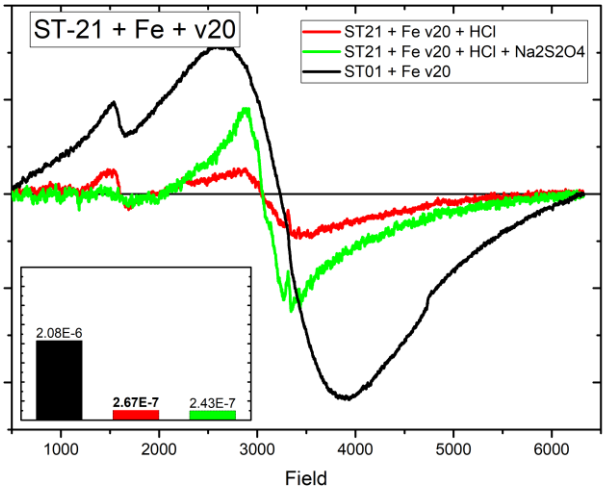

Figure S13 EPR spectra of samples prepared from ST-21 at different stages of the process, vacuum dried at room temperature. The inset shows the magnetic susceptibility of the sample.

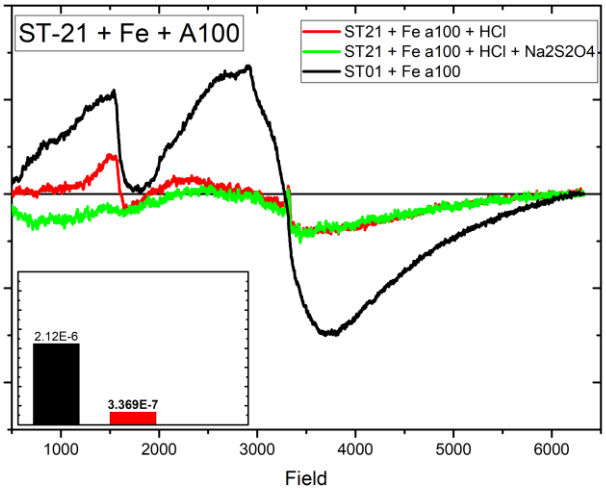

Figure S14 EPR spectra of samples prepared from ST-21 at different stages of the process, vacuum dried at 100° C. The inset shows the magnetic susceptibility of the sample.

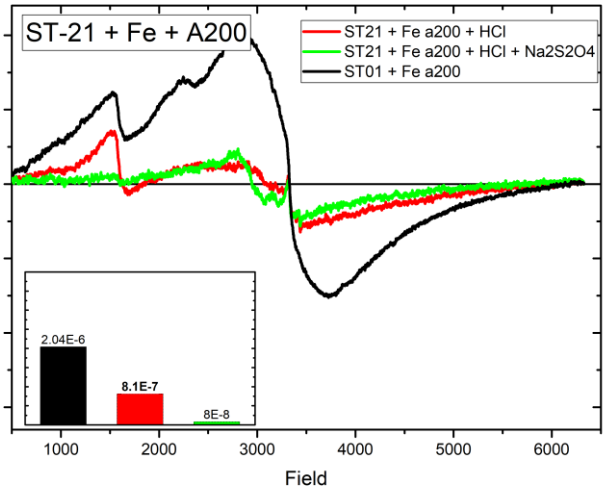

Figure S15 EPR spectra of samples prepared from ST-21 at different stages of the process, vacuum dried at 200° C. The inset shows the magnetic susceptibility of the sample.

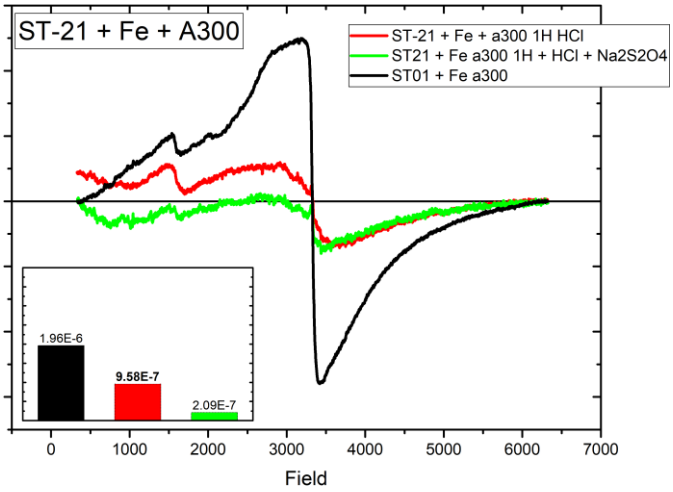

Figure S16 EPR spectra of samples prepared from ST-21 at different stages of the process, vacuum dried at 300° C. The inset shows the magnetic susceptibility of the sample.

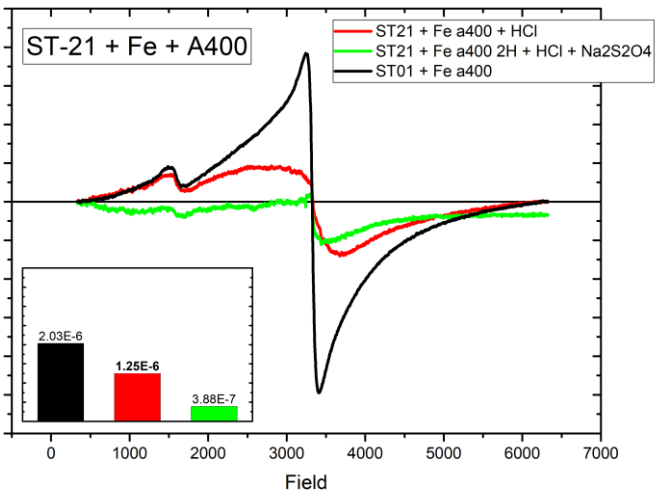

Figure S17 EPR spectra of samples prepared from ST-21 at different stages of the process, vacuum dried at 400° C. The inset shows the magnetic susceptibility of the sample.

5. Assessing the reproducibility of the sample preparation procedure

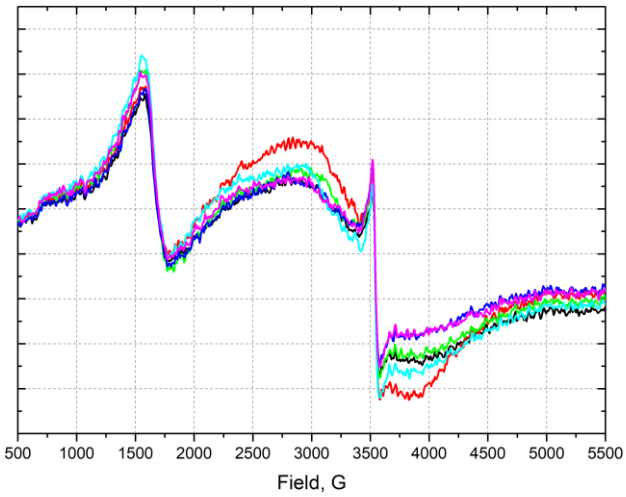

Figure S18 EPR spectra of iron ion deposited TiO_2 ST-01 samples. The EPR signal near 3500 G in initial samples, presumably, can be attributed to small foreign impurity, e.g., Fe because of preparation procedure.

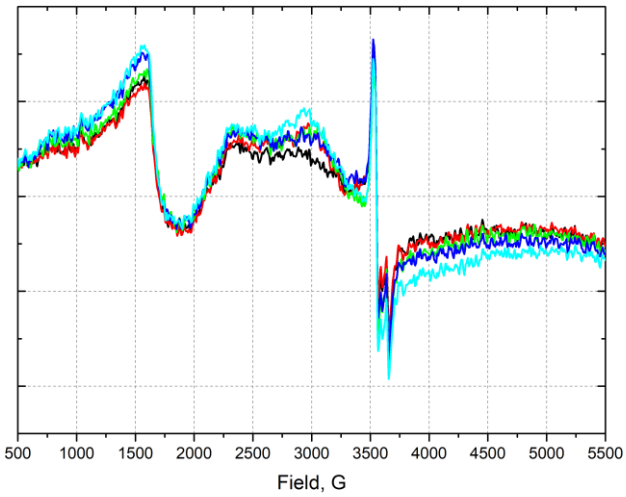

Figure S19 EPR spectra of iron ion deposited samples TiO_2 ST-21.

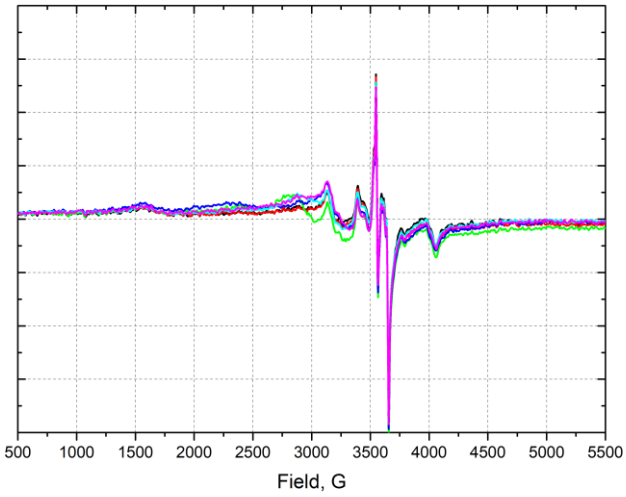

Figure S20 EPR spectra of iron ion deposited samples TiO_2 ST-41

6. The elaxed structures of TiO_2 used for DFT calculation.

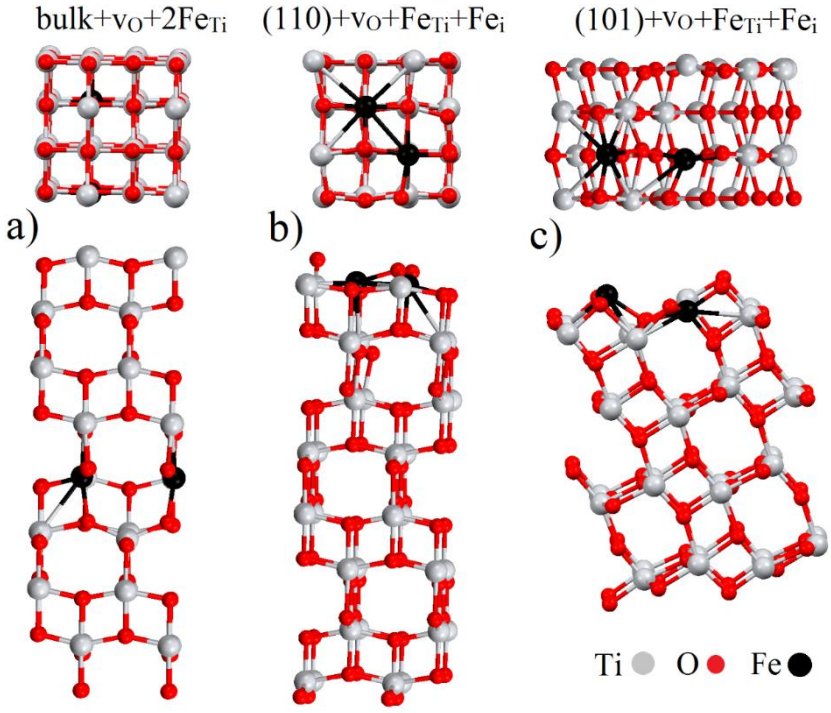

Figure S21 Top and side views of two substitutional iron impurities in core TiO_2 with oxygen vacancy between defects (a) and pair of substitutional and interstitial impurities in the vicinity of oxygen vacancy in (110) and (101) surfaces, (b) and (c) respectively.